Chapter 5

Enhanced Biomass Production And Bioremediation of *Diplosphaera mucosa VSPA* Using Simulated Raceway Reactor

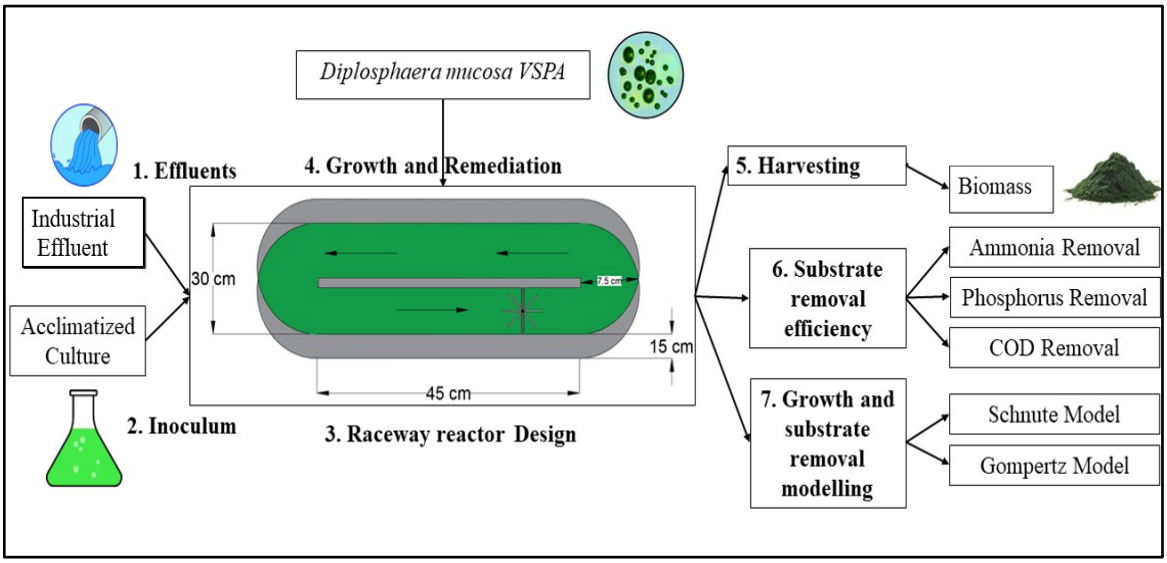

Enhanced Biomass Production and Bioremediation of *Diplosphaera mucosa VSPA* Using Simulated Raceway Reactor

5.1. Introduction

The current study reports the treatment efficiency of industrial waste effluent (IWE) by *D. mucosa VSPA*. The treatment efficiency of *D. mucosa VSPA* was compared with *C. pyrenoidosa,* as both belong to the same class, *Trebouxiophyceae*. Also, many previous studies have reported the application of C. *pyrenoidosa* for wastewater treatment [320], [321]. The treatment process was carried out in lab scale simulated open raceway bioreactor. The value addition of the treatment process was determined in terms of microalgae biomass productivity. After that, experimental results were simulated and validated using both three-parameters and four-parameter growth models.

5.2. Materials and Methods

5.2.1. Strain Isolation and Characterisation

A *Diplosphaera mucosa* strain was isolated from the inlet sewage treatment plant (STP) in Bhagwanpur, Varanasi, India (25° 18' 0" N, 82° 55' 48" E). The sample was serially diluted and spread on agar plates containing Bold Basal Media (BBM) (Bischoff 1963). Plates were kept in an incubator at 25ºC and illuminated at 2500 lux intensity using LED tubes. Single colonies were picked up by examination under a microscope and streaked on fresh plates. The streaking process continued until pure culture (free from contamination, confirmed under the microscope, **figure 5.1**) was obtained. The sequence of the isolated culture was identified by 18s rRNA sequencing and analysed by the BLAST program. After that, the phylogenetic tree was constructed using MEGA 11. The sequencing process was assisted by the National Collection of Industrial Microorganisms (NCIM), National Chemical Laboratory (NCL), Pune, India. *Chlorella pyrenoidosa* strain (NCIM accession no. 2738) was also procured from the NCIM. The supplied culture was revived in Bold Basal Medium

(BBM) [322] in Erlenmeyer flasks. Flasks were incubated at 25°C with a 120-rpm shaking speed. Flasks were illuminated by LED tubes at 2500 lux intensity. pH was monitored daily and adjusted at pH 7 by using 1 N HCl because the pH of the media increased during microalgae growth [323].

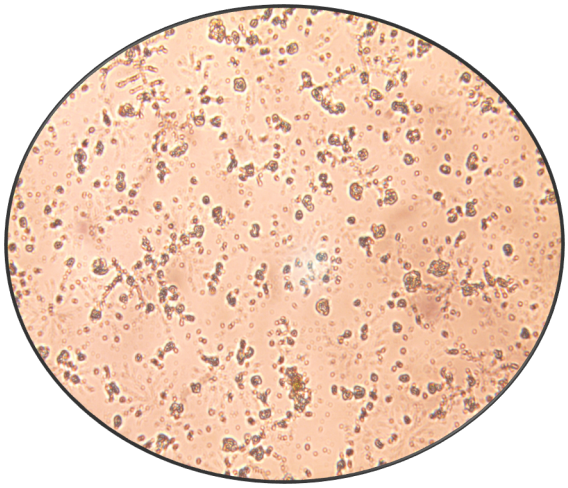

Figure 5.1. Microscopic image of the isolated *D. mucosa VSPA* strain (Taken under 40X Resolution)

5.2.2. Industrial Waste effluent collection and Characterisation

Industrial waste effluent was collected in a black bottle from the desalter unit of the refinery unit located in Mathura, India (27° 22' 48" N, 77° 40' 48" E). The Mathura Refinery was established in 1982 and can produce 8 MMTPA (millions of metric tonnes per annum) of oil, supplying a significant part to the NCR region [324]. The temperature of the IWE was measured by a digital thermometer at the collection site, sealed immediately, and packed with dry ice. After that, bottles were opened directly in the lab, filtered using Whatman filter paper (45mm), and immediately stored at 4°C for further use. The characterisation of the IWE was performed according to internationally recognised procedures, as indicated in **Table 5.1**[299].

Table 5.1. Industrial waste effluent characterisation performed using standard procedures.

S.No.	Parameter	Value
1.	Colour (Visual)	Dark Black
2.	pH	8.6
3.	Temperature (^{0}C)	39
4.	Total suspended solids (mg/L)	310
5.	Total dissolved solids (mg/L)	2100
6.	Total Solids (mg/L)	5200
7.	Turbidity (NTU)	380
8.	Chloride (Cl^-) mg/L	782
9.	Alkalinity (carbonate) (mg/L)	38.4
10.	Phenol (mg/L)	1.54
11.	Nitrogen (ammonia) (mg/L)	55.6
12.	Nitrogen (Nitrate) (mg/L)	8.6
13.	Phosphate (mg/L)	3.8
14.	N/P ratio	14.47
15.	Dissolved oxygen (mg/L)	1.5
16.	BOD_5 (mg/L)	344.4
17.	COD (mg/L)	1220
18.	Total organic carbon (TOC) (mg/L)	392
19.	Color (Hazen)	190

5.2.3. Raceway Reactor Design

Due to the raceway pond's easy design and scalability, IWE treatment was carried out in lab scale raceway bioreactor constructed using Perspex sheets, as shown in Figure 5.2(A). A raceway bioreactor is an open pond system typically designed in a shallow, oval or looped channel configuration, where microalgae are cultivated under natural or artificial light. The culture is mixed using a paddle wheel to ensure even light exposure and nutrient distribution. It is widely used for large-scale, cost-effective microalgal biomass production.

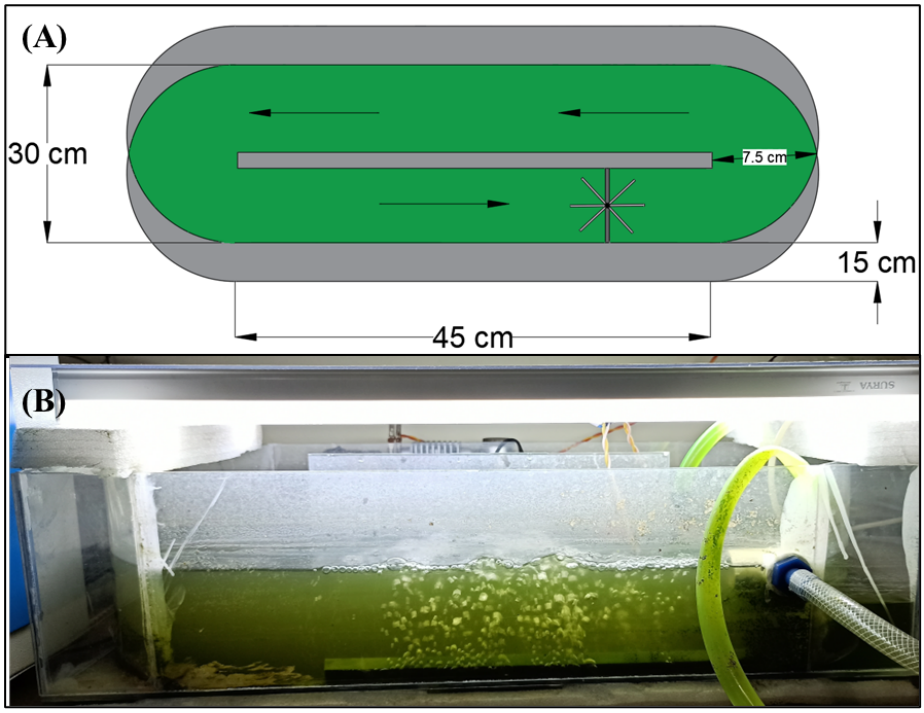

Figure 5.2. (A) Design of the raceway bioreactor used for the treatment of petroleum effluent. (B) Experimental set-up of the raceway pond treating petroleum effluent.

The total volume of the reactor was approximately 23 L, with a working volume of 15 L. A channel in the reactor was created using a 2 cm thick divider wall placed at the centre of the pond. The reactor was mixed with the help of a paddle wheel that was fixed on one side and had four blades that rotated at 30 rpm thanks to a motor. The reactor was illuminated by two 25-watt LED tube lights placed at each side of the divider wall and at

the height of 20 cm from the bottom of the reactor, which supplied 2500 lux intensity of light to the growing culture.

5.2.4. Batch Treatment

In a raceway bioreactor, IWE was treated in batches, and the efficiency of ammonium nitrogen, phosphate phosphorus, and COD removal by both species was measured (Figure 5.2(B)) No prior acclimatisation of the species was done in IWE. The process's value addition was calculated using biomass productivity. For preparing inoculum or starter culture, species were cultivated in a 2 L flask with 1.5 L BBM media (10% of the raceway reactor's working volume). Cultivation was continued until cultures reached the mid-log phase, as determined by measuring optical density at 680 nm. This step was necessary to maintain a uniform biomass concentration at the start of the treatment process. Prepared cultures were used to inoculate the IWE-filled reactor. After inoculation, the paddle wheel was started at 30 rpm, and the reactor was illuminated at 2500 lux with a 16-hour photoperiod. The light intensity was measured using a lux meter, and it was approximately 4500 ± 200 lux on both sides of the reactor [325]. Various studies have reported that a photoperiod of 16 hours (16:8 light/dark cycles) positively impacts microalgae growth instead of the natural photoperiod, i.e., 12 hours [300], [301]. Distilled water was supplied in the reactor to maintain the volume level left after each sampling, which may be altered due to evaporation. However, the supply of distilled water was not required daily, and the total supplied amount was 70-80 ml [326]. Treatment was continued until the stationary phase was reached, which was evaluated by measuring the absorbance of samples withdrawn daily from the reactor. Samples were also examined under the microscope to monitor the contamination. The reactor was also operated without an inoculum, which served as a blank. The treatment process was performed in triplicate, and average values were used for further calculation.

5.2.5. Analytical Techniques

Every day, 100 ml of a sample was taken from the reactor to determine the biomass, and remaining substrate concentrations. Analysis was done using spectrophotometric and colorimetric methods.

5.2.5.1. Biomass concentration determination

The Biomass concentration (Conc.) of the withdrawn sample was determined by measuring its optical density (OD) at 680 nm and calculating the value by Eq. (5.1) [327]:

$$OD = 0.1324 \times Conc. \qquad (R^2 = 0.98) \qquad (5.1)$$

During biomass measurement, IWE was used as a blank for cancelling the black colour of IWE or any other background noise [328]. The relationship (Eq. (5.1)) between OD and biomass concentration was determined by plotting an optical density curve of different dilutions of known biomass concentration. After determining the biomass concentration, the sample was centrifuged at 6000 rpm for 10 minutes. The supernatant was collected for substrate analysis, and the biomass pellet was collected separately for further analysis.

5.2.5.2. Substrate concentration determination

The supernatant collected after centrifugation was used to determine the remaining concentrations of ammonium nitrogen (NH_4^+-N), phosphate phosphorus (PO_4^{3-}-P), and chemical oxygen demand (COD). NH_4^+-N concentration was determined by the phenate colorimetric method, and PO_4^{3-}-P concentration was determined by the vanadomolybdophosphoric acid method. COD was determined through the close reflux titration method [299]. The final removal efficiency (RE) of the substrates was determined by Eq. (5.2):

$$RE = \frac{S_o - S_f}{S_o} \times 100 \qquad (5.2)$$

where, S_o and S_f indicate the initial and final substrate concentrations (mg/L). The initial substrate concentration was measured just after the inoculation of the culture.

5.2.6. Growth modelling

Various sigmoidal mathematical models such as Logistic, Gompertz, Schnute, Richards, and Stannard were used for simulating microalgae growth [329]. Equations for these models are presented in **Table 5.2.** These mathematical models have kinetic constants or parameters that can be transformed into biological constants such as lag time, maximum specific growth rate, degradation rate, and asymptotic values. Logistic and Gompertz are three parameter models widely used for simulating microbial growth. The other three models, Schnute, Richards, and Stannard, are four-parameter models [329]. Due to their complex nature, they were used in fewer studies than Logistics and Gompertz.

Table 5.2. Mathematical model equations.

S.No.	Model	Model Equations	Reference
1	Logistics	$x = \frac{A}{\left\{1 + exp\left[\frac{4\mu}{A}(\lambda - t) + 2\right]\right\}}$	[329]
2	Gompertz	$x = Aexp\left[-exp\left\{\left(\frac{\mu e}{A}\right)(\lambda - t) + 1\right\}\right]$	[329]
3	Schnute	$x = \left(\mu\frac{(1-b)}{a}\right)\left[\frac{1 - bexp(a\lambda + 1 - b - at}{1-b}\right]^{\left(-\frac{1}{v}\right)}$	[329]
4	Richards	$x = A\left\{1 + vexp(1+v)exp\left[\frac{\mu}{A}(1 + v)\left(1 - \frac{1}{v}\right)(\lambda - t)\right]\right\}^{\left(-\frac{1}{v}\right)}$	[329]
5	Stannard	$x = A\left\{1 + vexp(1+v)exp\left[\frac{\mu}{A}(1 + v)\left(1 + \frac{1}{v}\right)(\lambda - t)\right]\right\}^{\left(-\frac{1}{v}\right)}$	[329]

x= biomass concentration, A = asymptote value, μ = specific growth rate, λ = duration of lag phase, t = time, v, a and b are constants.

5.2.7. Statistical Analysis

After performing experiments in triplicate, average values of biomass concentration were used to simulate the model. A Student's paired t-test was applied to determine whether the differences between the tested cultures were significant or not. A t-test was carried out using Origin Lab (Version 217) at a significance level of 0.05. A solver supplement of Microsoft Excel (Version 2016) was used for solving the models and determining the model parameters. The best model was selected based on three criteria. Akaike's information criterion (AIC), corrected Akaike's information criterion (AICc), and Bayesian information criterion (BIC), represented by Eq. (5.3) to Eq. (5.5) [330]. All these criteria were computed using the university edition of SAS software (online version).

$$AIC = -2\log(\sigma^2) + 2r \quad (5.3)$$

$$AICCc = -2\log(\sigma^2) + 2\frac{rT}{(T-r-1)} \quad (5.4)$$

$$BIC = -2\log(\sigma^2) + 2r\ logT \quad (5.5)$$

where, σ^2 is the most probable variance estimate, r indicates the number of independent parameters and T is the sample size.

5.3. Results and Discussion

5.3.1. Strain Identification

18s rRNA gene sequencing was performed for the identification of the strain. The obtained sequence was analysed using BLAST. The BLAST analysis revealed that the strain is closely related to *Diplosphaera mucosa* (91%), therefore it is named *Diplosphaera mucosa* VSPA. MEGA 11 was used to construct the phylogenetic tree and perform the evolutionary analysis. The UPGMA method was used to infer evolutionary history [331]. The optimal tree is shown in **Figure 5.3.** The evolutionary distances were determined using the Maximum Composite Likelihood technique, and they are measured in base substitutions per site [332].

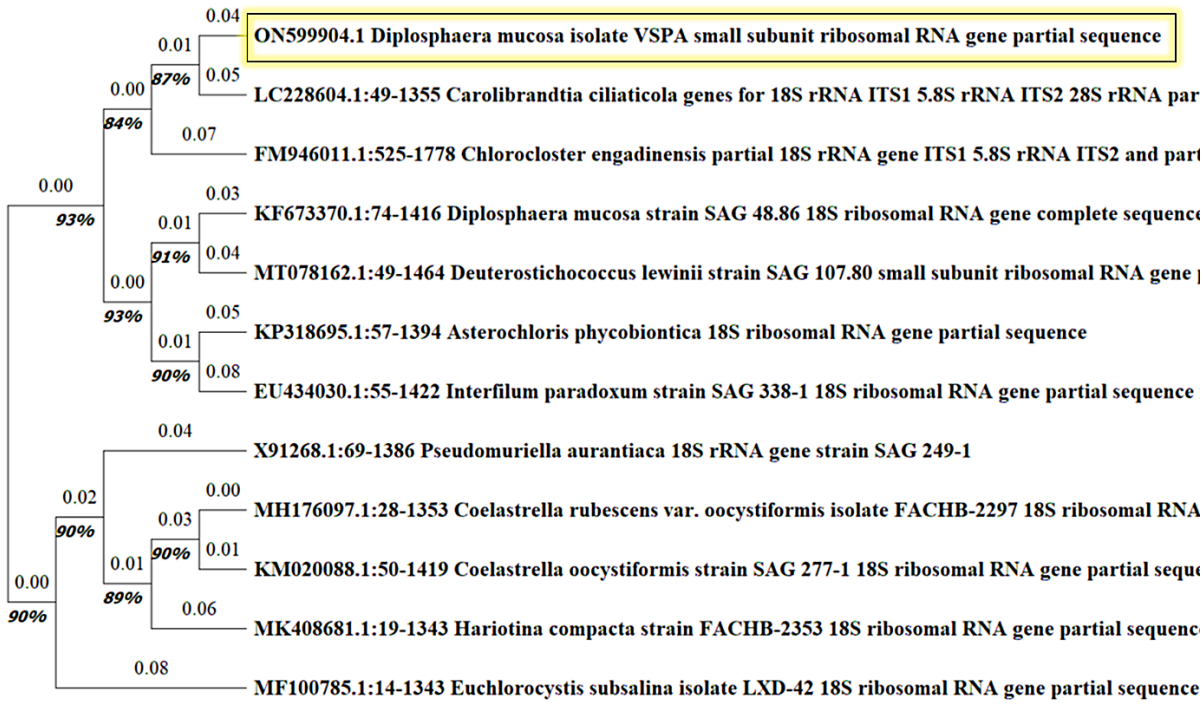

Figure 5.3 Optimal tree structure representing the isolated strain generated after phylogenetic tree analysis.

5.3.2. Biomass production

As the demand for energy and freshwater is increasing day by day; therefore, there is a need to develop technologies that can treat wastewater and generate green energy. The value added of the current treatment process was assessed in terms of biomass production. Microalgae have evolved their systems and metabolic pathways to produce more biomass with less conversion efficiency, somewhere between 2% and 6% photosynthetic efficiency in fixing CO_2, and between 5% and 10% allocated carbon to synthesise fuels and chemicals in natural conditions because these conditions are not necessary for cultivation [333]. Microalgae growth was accessed in terms of biomass concentration, as indicated in **Figure 5.4.**

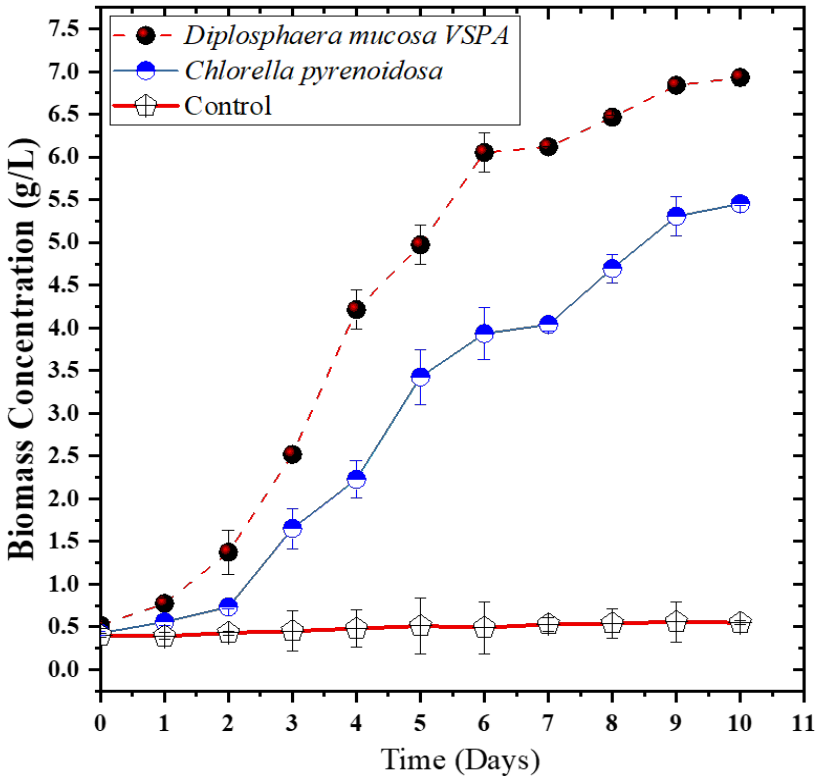

Figure 5.4. Biomass concentration profile during the cultivation of *D. mucosa VSPA* and *C. pyrenoidosa* in IWE.

It is evident from Figure 4 that *D. mucosa* VSPA grew faster in comparison to *C. pyrenoidosa* ($p < 0.05$). As no prior acclimatisation was performed, therefore, approximately a 1-day lag phase was noticed in *D. mucosa* VSPA culture, while a 2-day lag phase was noticed in *C. pyrenoidosa* culture. During the lag phase, microalgae adapt to the unfavourable environment of wastewater through various physiochemical changes, such as synthesising enzymes needed to assimilate substrates and degrade toxic compounds present in the wastewater [334]. IWE has a high amount of phenol and hydrocarbon concentrations that may affect microalgae growth during the initial stage, increasing the lag phase duration. However, microalgae can degrade phenolic compounds and hydrocarbons by synthesising the enzymes required for the degradation of these compounds and increasing their growth rate [335]. The isolation of *D. mucosa VSPA* from sewage treatment plants may have lowered its acclimatisation period, as the species was exposed to various

pollutants for many generations. Natural selection might favour rapid strains over fewer rapid strains for their survival. It may have developed a more rapid response for degrading toxic compounds, as sewage has a significant number of phenolic compounds [336]. This was also concluded in a study by Maheshwari et al. (2019), where they isolated potent microalgae strains from sewage [337]. After the lag phase, both cultures started growing at a faster rate until day 9, when they reached the stationary phase. The growth rate of *D. mucosa VSPA* was high, achieving a final biomass concentration of 6.93 g/L after 10 days of cultivation. *C. pyrenoidosa* also performed well in IWE, with the final biomass concentration reaching 5.43 g/L. There can be two possible reasons for achieving such a high biomass concentration in IWE: a high concentration of NH_4^+-N and a high N/P ratio (14.47). NH_4^+-N is one preferable nitrogen source microalgae as they require less energy to assimilate it, as discussed in more detail in the upcoming section. As per Redfield's investigation, the typical microalgal biomass has the stochiometric formula $C_{106}H_{181}O_{45}N_{16}P$. Various biomass characterization analyses, such as ash analysis and CHNS analysis, were performed in previous studies that confirmed the mentioned the stochiometric formula of biomass [338], [339]. Therefore, the N/P ratio of the medium should be around 16:1 or more for high microalgal growth [340]. The N/P ratio of IWE was 14.47:1, near 16:1, supporting the production of a high biomass concentration. Mayers et al. (2014) studied the effects of different N/P ratios ranging from 16:1 to 80:1 on the growth of *Nannochloropsis* sp. High biomass productivity was achieved at N/P ratios of 16:1 and 32:1 [315]. At the same time, productivity decreased at 64:1 and 80:1. In another study, *Chlorella* sp. biomass productivity became nil when the N/P ratio decreased below 5:1 [341]. The D. mucosa *VSPA* strain also performed well compared to the biomass concentration reported in previous studies. Das et al. (2018) cultivated *Chlorella* sp. and

Scenedesmus sp. in 1 L PBR-treated petroleum effluent, with a final biomass concentration of 1.72 g/L [342].

5.3.3. Substrate removal efficiency

Various pollutants, such as nitrogen, phosphorus, organic carbon, and macro- and micro-elements, are present in wastewater. Nitrogen is present in the form of ammonium nitrogen, nitrate, nitrite, and organically bound nitrogen, and phosphorus is present in the form of orthophosphate. These pollutants act as nutrients for microalgal growth, converting them into useful biomass [343]. In the present treatment process, the removal of NH_4^+-N, PO_4^{3-}-P, and COD from IWE by both species was accessed. The removal efficiency of all tested pollutants (NH_4^+-N, PO_4^{3-}-P, and COD) obtained by *D. mucosa VSPA* was 10% higher than that obtained by *C. pyrenoidosa.*

5.3.3.1. Ammonium-nitrogen (NH_4^+-N) removal

Microalgal cells have developed a preference for assimilating nitrogen in the form of ammonium-nitrogen (NH_4^+-N) rather than nitrate or nitrite due to the lower energy requirement for the uptake of NH_4^+-N. This strategic choice allows microalgae to optimize their nitrogen utilization and conserve valuable cellular energy resources. To facilitate the efficient uptake of NH_4^+-N from their surroundings, microalgae employ specialized proteins known as ammonium transporters. These transporters act as molecular gateways, enabling the selective uptake of NH_4^+-N into the cellular interior. Once inside the cell, NH4+-N serves as a critical precursor for the synthesis of various nitrogen-containing compounds. Notably, during amino acid biosynthesis, NH_4^+-N plays a central role in the production of glutamine. Glutamine is an essential amino acid that participates in numerous cellular processes, including protein synthesis and nitrogen storage. The utilization of NH_4^+-N for glutamine synthesis represents an integral part of microalgae's metabolic strategy to efficiently harness nitrogen resources for growth and survival. This process has

been studied and documented by researchers, as exemplified by the work[344], which highlights the significance of the ammonium transporter and its role in microalgal nitrogen assimilation. The NH_4^+-N removal profile by both species is represented in **Figure 5.5**.

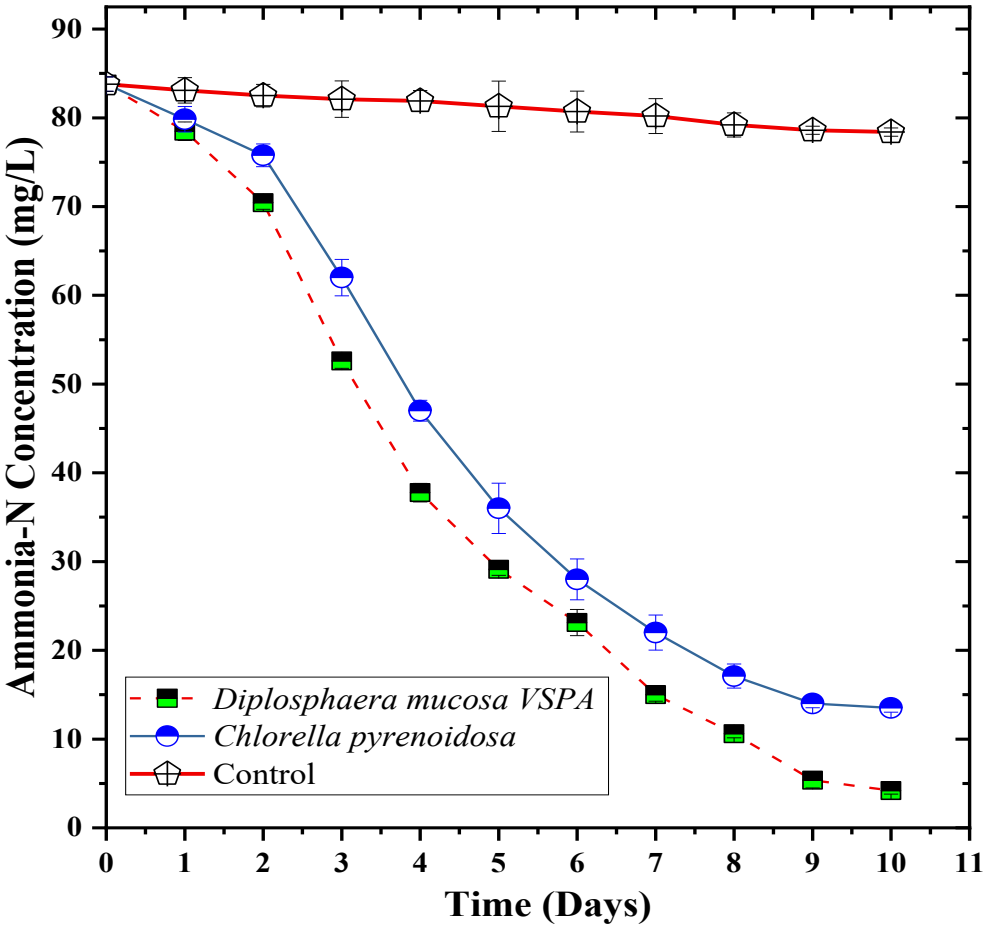

Figure 5.5. Ammonium nitrogen removal profile by both species from IWE. *D. mucosa VSPA* strain remediated 94.99% of NH_4^+-N, with the final concentration reaching 4.19 mg/L in the raceway reactor, greater than *C. pyrenoidosa* ($p < 0.05$). In contrast, *C. pyrenoidosa* removed only 83.89% of NH_4^+-N, with a final concentration reaching 13.50 mg/L.

The removal pattern was similar to the growth of the microalgae species, indicating that the removal of pollutants depends on microalgae growth. After 1-2 days, when the lag phase was over, NH_4^+-N was rapidly removed by both species until day 10 because it is the preferred nitrogen source assimilated by microalgae. As raceway ponds are open reactors,

bacterial contamination is possible [345]. Hence, it is possible that some percentage of NH_4^+-N may be removed due to biological processes, such as bacterial nitrification, or physical processes, such as volatilization or sedimentation [346]. But, in the control experiment, only 6.44% of NH_4^+-N was removed, indicating that microalgae were solely responsible for removing a significant portion of NH_4^+-N. A similar removal efficiency was obtained during the cultivation of *Chlorella* sp. in petroleum effluent with nearly similar nitrogen concentrations but after 15 days of cultivation [342].

5.3.3.2. Phosphate phosphorus removal

Phosphorus is a common constituent of wastewater and is predominantly present in the form of orthophosphate (PO_4^{3-}). Microalgal cells have a remarkable ability to actively transport and absorb this orthophosphate from the surrounding environment. Once inside the cells, PO_4^{3-} is utilized in the synthesis of various essential organic compounds, including adenosine triphosphate (ATP), through distinct processes such as substrate-level phosphorylation, oxidative phosphorylation, and photo-phosphorylation [347]. Furthermore, certain microalgal species exhibit an intriguing mechanism to cope with excess - PO_4^{3-} -P in their environment. They store this surplus phosphorus in their vacuoles in the form of polyphosphate granules. This accumulation serves as a reserve for times when phosphorus becomes limited, allowing the microalgae to tap into these stored polyphosphate reserves and sustain essential cellular processes under phosphorus-deficient conditions[348]. The PO_4^{3-}-P assimilation profile by both species has been indicated in **Figure 5.6.**

In this case, also, *D. mucosa VSPA* removed the highest amount of PO_4^{3-}-P compared to *C. pyrenoidosa* ($p > 0.05$) during the 10-day cultivation period. *D. mucosa VSPA* remediated 78.97% of PO_4^{3-}-P, with the final concentration reaching 0.82 mg/L. In comparison, *C. pyrenoidosa* removed 64.94% of PO_4^{3-}-P with a final concentration

reaching 1.25 mg/L. The removal efficiency of PO_4^{3-}-P by both species was not high as compared to ammonium nitrogen because of the straightforward fact that the requirement of nitrogen by microalgae is higher; in contrast, only 1% (by weight) phosphate is present in algae biomass [349]. Previous studies have also reported that microalgae species assimilate nitrogen more efficiently than phosphorus. Similar to the case of NH_4^+-N, some portion of PO_4^{3-}-P may be eliminated due to some physical processes, such as chemical precipitation [348]. However, only 14.10% of PO_4^{3-}-P was eliminated in the control experiment, indicating that microalgae assimilated a significant portion of phosphate. The removal efficiency obtained was greater than that obtained in previous studies. During the cultivation of mixed microalgal species in rotating biofilm reactors, 50% and 55.6% PRE were obtained at 24hr and 48hr HRT, respectively, during a period of 12 weeks. There was no significant increase in removal efficiency upon increasing HRT [350].

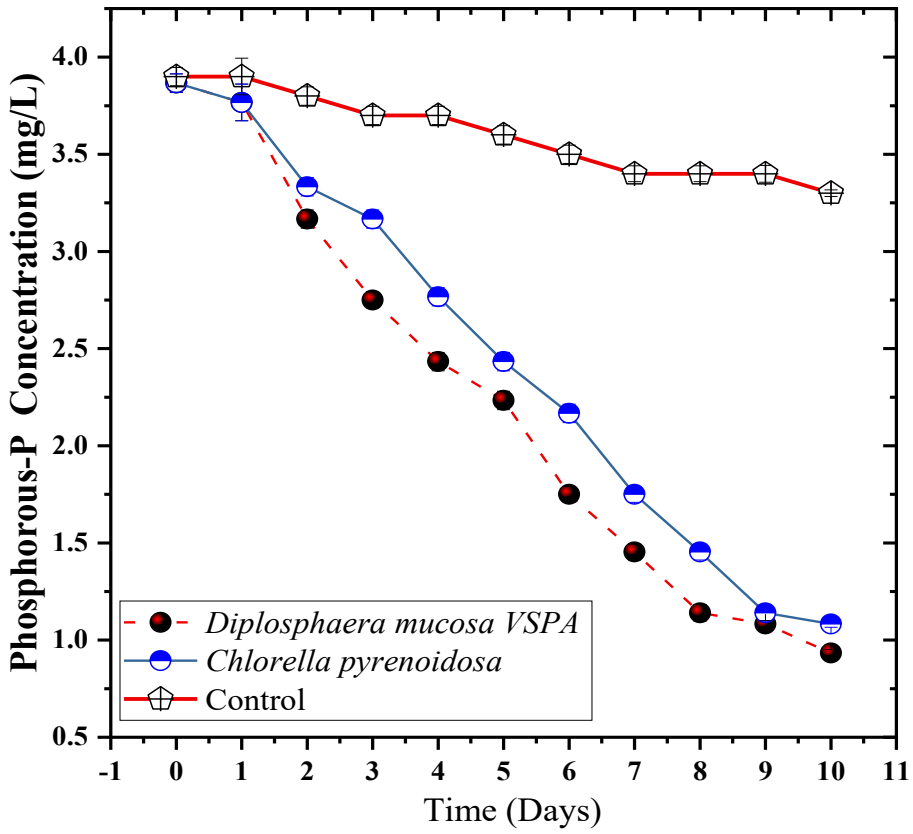

Figure 5.6. Phosphate phosphorus removal profile by both species from IWE.

5.3.3.3. Chemical oxygen demand (COD) Removal

Chemical oxygen demand (COD) is a critical parameter in wastewater treatment as it quantifies the organic load or strength of the wastewater. Specifically, COD represents the amount of oxygen required for the complete oxidation of the organic substances present in the wastewater [351]. While the fate of other common nutrients like nitrogen and phosphorus during microalgal-based wastewater treatment has been extensively studied, the behavior of COD in this context remains less characterized. Understanding the dynamics of COD during microalgal-based wastewater treatment is crucial for the efficient design and operation of such systems. The ability of microalgae to perform mixotrophic cultivation in response to elevated organic content opens up intriguing possibilities for enhancing wastewater treatment efficiency and resource recovery. However, further research and comprehensive studies are needed to fully elucidate the intricate interactions between microalgae and the COD present in wastewater, thereby optimizing the overall performance of microalgal-based treatment processes. The pattern of COD removal from IWE is represented in **Figure 5.7.**

In contrast to the above discussion, both species were highly efficient at removing COD from IWE. *D. mucosa VSPA* removed 92.67% of COD, with a final concentration reaching 90 mg/L, higher than *C. pyrenoidosa* ($p < 0.05$). *C. pyrenoidosa* removed 81.27% of COD, with a final concentration reaching 6.59 mg/L. It is evident that as the culture reaches the stationary phase, the COD of the sample will increase due to the release of organic materials by microalgal cells. But high removal efficiencies in both cultures indicated that newly growing microalgal cells may have assimilated released organic content or that some COD may be remediated by bacterial contamination, as indicated in the control. As there is a direct relationship between COD and TOC (total organic carbon), authors have also reported COD removal efficiency in terms of TOC removal efficiency.

Das et al. (2019) cultivated *Chlorella* sp. in petroleum effluent using 1 L of PBR. *Chlorella* removed 73% of TOC within 15 days [342].

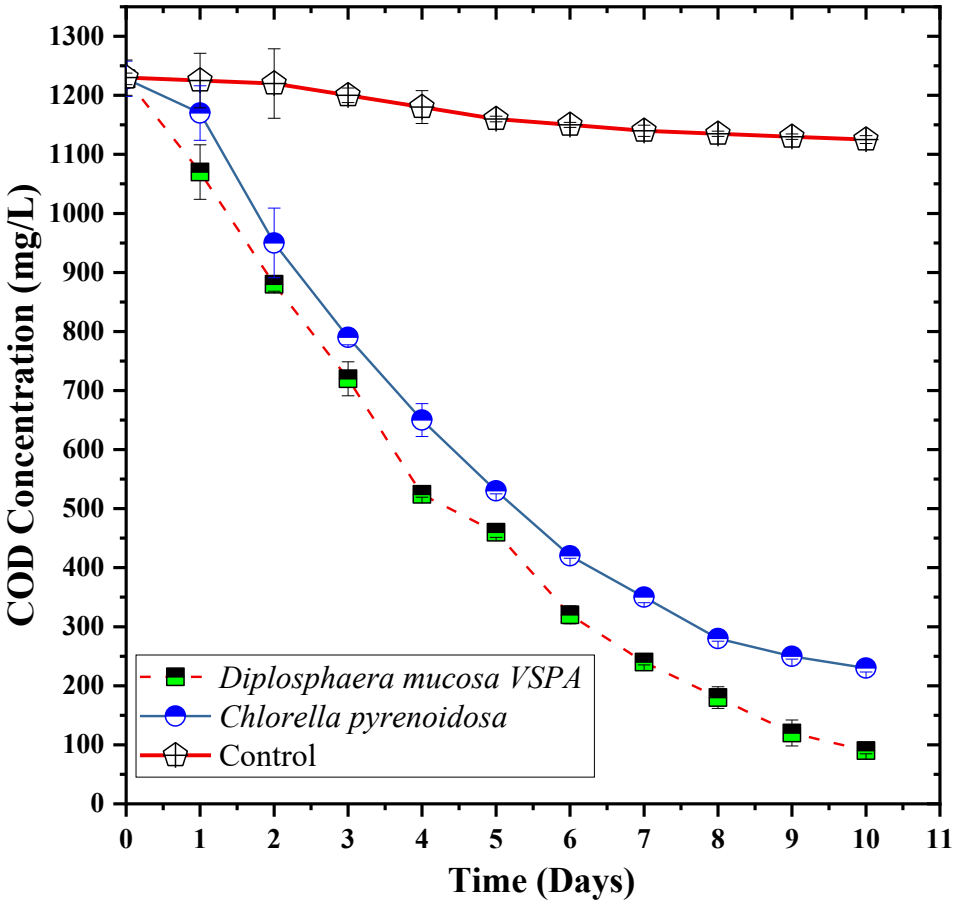

Figure 5.7. Chemical oxygen demand (COD) removal profile by both species from IWE.

5.3.4. Growth Kinetic Modelling

Mathematical modelling is a valuable tool for predicting the growth pattern of microalgae in wastewater and determining some functional parameters, such as the duration of the lag phase, the maximum specific growth rate, and the final biomass concentration. Also, they can verify the experimental results. Some other model parameters determined at the lab scale can assist in scaling up the process to a larger scale [343]. Two three-parameter models, Logistic and Gompertz, and three four-parameter models (Schnute, Richards, and

Stannard) were used for simulating the experimental results for both species, as shown in **Figure 5.8.**

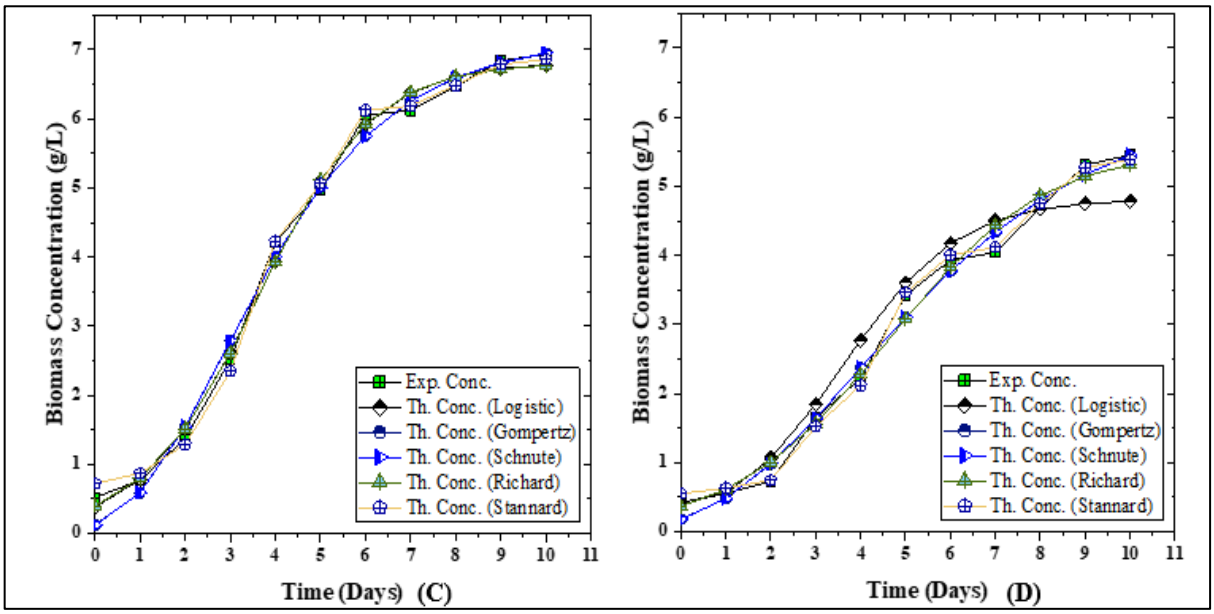

Figure 5.8. Predictive modelling of biomass production using various kinetic models in IWE: Biomass production by (C) *D. mucosa VSPA*, (D) *C. pyrenoidosa*.

The logistic (Verhulst) model, first put forth in 1838 to explain population expansion, is now frequently employed to explain microbial cell growth in various biological systems [352]. This model doesn't take substrate inhibition into account. Instead, it shows how the number of microorganisms changes over time as a function of their growth rate, initial biomass, maximum biomass concentration, and time [353]. The Gompertz's function was first applied to represent the distribution of ages in human populations, and it was then modified and applied to simulate microbial growth. The model represents growth as a function of time, biomass productivity, and maximum biomass concentration (Eifert et al. 1994). The Schnute curve has three distinct phases that contribute to its characteristics: an initial lag or slow growth phase, a phase of fast exponential growth, and a phase of slower growth. Numerous scientific disciplines, such as population dynamics, bacterial growth, population ecology, plant biology, chemistry, and statistics, use the Schnute

function [355]. Richard's model performs better in some situations to describe the microbial growth curve. Richard's function has a parameter called m (maintenance coefficient) that describes the form of other sigmoid functions and general three-parameter functions. Significantly, the Richards model allows determining the biomass value from growth curves measured by absorbance with greater accuracy than the Gompertz and other exponential models, allowing lag time determination from the individual absorbance growth curve [356]. Stannard's model appears somewhat similar to Richard's model, with the same assumptions. The difference between these two occurred during the derivation process from Schnute's model [329]. The best model was computed based on some model evaluation criteria, as shown in **Figure 5.9 and 5.10** and **Table 5.3**. The values of biological parameters and kinetic constants obtained after simulating experimental data using all models are also represented in **Table 5.3**.

Table 5.3. Values of biological parameters and model evaluation criterions obtained after simulating the experimental data on the growth models.

Species	***D. mucosa VSPA***							***C. pyrenoidosa***						
	Biomass Production													
Models	**Model parameters**			**Model evaluation criterions**				**Model parameters**			**Model evaluation criterions**			
	A (g/L)	**μ_m (d^{-1})**	**λ (d)**	**R^2**	**AIC**	**AICC**	**BIC**	**A (g/L)**	**μ_m (d^{-1})**	**λ (d)**	**R^2**	**AIC**	**AICC**	**BIC**
Logistic	6.82	1.33	1.05	0.93	27.12	30.55	28.31	4.81	0.63	0.63	0.92	19.31	22.74	20.5
Gompertz	7.17	1.28	0.83	0.94	25.38	28.8	26.57	6.26	0.74	0.81	0.98	1.46	4.89	2.65
Schnute	7.21	1.27	0.81	0.94	25.29	28.29	26.48	6.23	0.74	0.8	0.98	1.3	4.73	2.5
Richard	6.81	1.07	1.06	0.92	27.19	30.62	28.39	5.54	1.04	1.16	0.97	7.03	10.46	8.23
Stannard	9.5	0.34	0.48	0.92	28.4	31.83	29.59	7.68	0.02	0.35	0.96	13.42	16.85	14.62

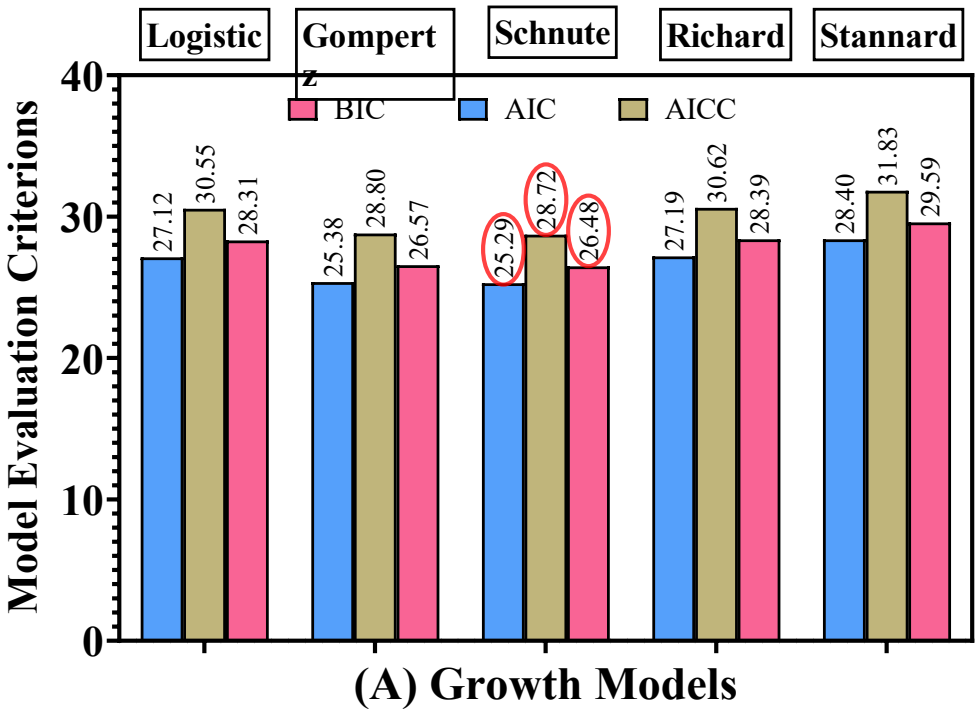

Figure 5.9. Values of model evaluation criterions (AIC, AICC & BIC) obtained after simulating experimental data on the growth model: Biomass production by *mucosa VSPA;* Smaller these values, more the accuracy of the model.

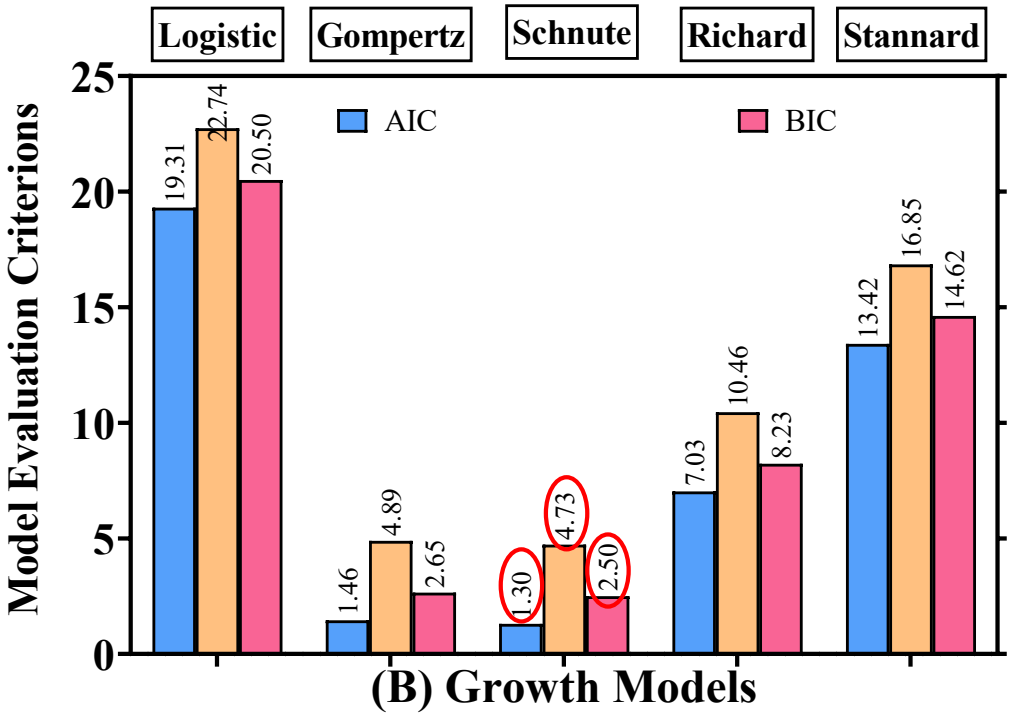

Figure 5.10. Values of model evaluation criterions (AIC, AICC & BIC) obtained after simulating experimental data on the growth model: Biomass production by *C. pyrenoidosa*; Smaller these values, more the accuracy of the model.

Models were compared based on three criteria: AIC, AICC, and BIC. The lower the values of these criteria, the more likely is that the models are best-fit models. Based on these criteria, the Schnute model was the best fit among all models for both species. The fitting of the four-parameter (Schnute) model was also supported during the growth of *Spirulina platensis* [355]. A good fit of the four-parameter model was also reported during the cultivation of *Chlorella vulgaris* in domestic wastewater for biodiesel production (Lam et al. 2017). The Gompertz model was better fitted among the three-parameter modes than the logistic model. The model criterion's values for the Gompertz mode were near those of the Schnute model and lower than those of the other two four-parameter models. If a more complex study is not required, then three-parameter models can be ideal, because they are simple in design, easier to use, and can easily reveal biological parameters. Various studies have reported the application of the Gompertz model for describing the biomass production by *S. platensis*, the growth of *Aphanothece microscopica*, and the co-culture growth of microalgae and cyanobacteria [358], [359]. Schnute and Gompertz models can be considered for further testing at the pilot scale in all cases. Other models also presented a good fit to the experimental data, but their results were not constant in some cases. The results of the Richard model were constant in most cases, but the results of the Stannard model were variable in most cases. Richard's model can also be considered for further testing at the pilot scale. The successful application of the Richard model for fitting experimental data generated during microalgae-based wastewater treatment processes was reported in some studies [357], [360].

Table 5.3 represents three biological parameters: maximum biomass concentration (A, g/L), lag duration (λ, days), and maximum specific growth rate (μ_m, d^{-1}) computed from both models. λ for both species was around 0.80 days, as computed by Gompertz and Schnute modes, respectively. At the same time, the Richard model predicted more than a

1-day lag duration for both species. Prior acclimatisation of microalgal species in IWE will help in the reduction of lag duration. Biomass production rates are measured in terms of maximum specific growth rate (μ_m). The maximum biomass production rate of *D. mucosa VSPA* was approx. 1.28 d^{-1}, 1.27 d^{-1} and 1.07 d^{-1}, while that of *C. pyrenoidosa* was 0.74 d^{-1}, 0.74 d^{-1} and 1.04 d^{-1} as predicted by Gompertz, Schnute, and Richard models, respectively. So, all three models indicate that *D. mucosa VSPA* has better adaptability in IWE for the same duration of the lag period. The Logistic and Stannard models also predicted the same situation. The prediction of μ_m through biological models will assist in determining the dilution factor (D) required for the operation of the large-scale continuous process. The D value should be less than μ_m to prevent cell washout during continuous operation. The next parameter, (asymptote, A), predicts the maximum yield of biomass by the microalgal species and determines the harvesting or stationary phase period. This parameter is typically used to increase productivity and study cell physiology in culture. As predicted by both models, maximum biomass concentration was achieved by *D. mucosa VSPA* species in comparison to *C. pyrenoidosa*. The prediction of harvesting time will provide an idea regarding the reactor's operation and deduce the overall cost of microalgae-based wastewater treatment. However, it should be noted that the current study was performed on a laboratory scale. So, a pilot scale study is needed further to test the model's applicability under varying conditions.

5.4. Conclusion

Analysis of the work indicates that *D. mucosa VSPA* treated IWE with high efficiency compared to *C. pyrenoidosa*, with a more than 10% difference in removal efficiency. The final biomass concentration in *D. mucosa VSPA* was also high, with a difference of more than 1 g/L compared to *C. pyrenoidosa*. A high N/P ratio of IWE supported high biomass productivity for both species. Among various models, Gompertz and Schnute's model

better fitted the experimental data generated during laboratory trials, suggesting that it can be further tested at a pilot scale. Therefore, as a conclusion, the future focus would be more on exploring species that grow in extreme conditions or less studied microalgae with other unique characteristics. They will easily acclimatise to toxic industrial effluents within a very short period and increase the efficiency of the microalgae-based wastewater process. Petroleum industries can set up cost-efficient large-scale raceway ponds near the refineries to treat effluent and decrease the load on freshwater bodies.